Extraction of the ^{12}C Longitudinal and Transverse Nuclear Electromagnetic Response Functions from Electron Scattering Cross Sections on Carbon

Arie Bodek,[1] M. E. Christy,[2] and Zihao Lin[1]

[1]*Department of Physics and Astronomy, University of Rochester, Rochester, NY 14627, USA**
[2]*Thomas Jefferson National Accelerator Facility, Newport News, VA 23606, USA*†

(Dated: October 26, 2023)

We report on an extraction of the ^{12}C Longitudinal ($\mathcal{R}_T(Q^2,\nu)$) and Transverse ($\mathcal{R}_L(Q^2,\nu)$) nuclear electromagnetic response functions from an analysis of all available electron scattering cross sections on carbon. The response functions are extracted for a large range of energy transfer ν (spanning the nuclear excitation, quasielastic, resonance regions and inelastic continuum) and for a large range of the square of the four-momentum transfer Q^2 ($0 < Q^2 < 1.2\ GeV^2$). The data sample consists of ≈6600 ^{12}C differential cross section measurements including preliminary high precision cross section measurements from Jefferson Lab Hall C experiment E-04-00. Since extracted response functions cover a very large range Q^2 and ν, they can be used to validate nuclear models as well Monte Caro generators for electron and neutrino scattering experiments.

****

Need to FIX: Yamaguchi data is in terms of Ex rather than ν. Ryan 180 deg datai data is in terms of Ex rather than ν. Remove Bounin 0.98 GeV 135 deg is FATOR OF 1.6 SMALLER THAN YAMAGUCHI Remove duplicate E04-001 data Remove E04-001 data with E0=1.2 GeV, Theta ¡30 deg (6 spectra) Get normalization of data set

I. INTRODUCTION

All electron scattering cross sections on nuclear targets can all be described in terms Transverse ($\mathcal{R}_T(Q^2,\nu)$) and Longitudinal ($\mathcal{R}_L(Q^2,\nu)$) nuclear electromagnetic response functions for each nuclear target. $\mathcal{R}_T(Q^2,\nu)$ and $\mathcal{R}_L(Q^2,\nu)$ are functions of the energy transfer ν and the the square of the 4-momentum transfer Q^2 (or equivalently as functions of momentum transfer bfq and excitation energy E_x). Theoretical models[1–5] can tested by comparing predictions of $\mathcal{R}_T(Q^2,\nu)$ and $\mathcal{R}_L(Q^2,\nu)$ to experimental data.

As summarized in Table I, a previous extraction of $\mathcal{R}_T(Q^2\nu)$ and $\mathcal{R}_L(Q^2,\nu)$ from experimental data in the quasielastic region was published in 1996 by Jourdan[6, 7] for values of momentum transfer of $\mathbf{q}$ of 0.30 GeV ($30 < \nu < 140$ MeV), 0.38 GeV ($30 < \nu < 210$ MeV), and 0.57 GeV ($50 < \nu < 340$ MeV). At the quasielastic peak these correspond to values of the square of the 4-momentum transfer Q^2 of 0.086 GeV^2 (ν=0.06 GeV), 0.134 GeV^2 (ν=0.10 GeV), and 0.285 GeV^2 (ν=0.20 GeV), respectively.

In the nuclear excitation region (excitation energy less than 40 MeV) $\mathcal{R}_T(Q^2\nu)$ and $\mathcal{R}_L(Q^2,\nu)$ were extracted in 1971 by Yamaguchi et. al. [8] for values of momentum transfer of $\mathbf{q}$ of 0.148, 0.1658, 0.2052, 0.2407 and 0.2078 GeV. For nuclear excitation energy of 25 MeV, these correspond to Q^2 values of 0.0208, 0.0269, 0.0409, 0.0570, and 0.0935 GeV^2, respectively.

In this communication we extract $\mathcal{R}_T(Q^2,\nu)$ and $\mathcal{R}_L(Q^2,\nu)$ from all available electron scattering data. The data sample consists of ≈10,000 ^{12}C differential cross section measurements (including preliminary high precision cross section measurements from Jefferson Lab Hall C experiment E-04-001). We report on extractions of $\mathcal{R}_T(Q^2,\nu)$ and $\mathcal{R}_L(Q^2,\nu)$ over a larger range of energy transfer ν (including the quasielastic, nuclear excitations, resonance region, and inelastic contiuum. in the range $0 < Q^2 < 1,2\ GeV^2$ (in Q^2 bins shown in Table I). Since the extracted response functions cover a very large range Q^2 and ν, they can be compared to recent nuclear models, and also validate Monte Caro generators for electron and neutrino scattering experiments,

II. INCLUSIVE ELECTRON-NUCLEON SCATTERING

In terms of the incident electron energy, E_0, the scattered electron energy, $E^{'}$, and the scattering angle, θ, the absolute value of the exchanged 4-momentum squared in electron-nucleon scattering is given by

$$Q^2 = (-q)^2 = 4E_0E^{'}\sin^2\frac{\theta}{2}, \tag{1}$$

the mass of the undetected hadronic system is

$$W^2 = M^2 + 2M\nu - Q^2, \tag{2}$$

and the square of the magnitude of 3-momentum transfer vector $\vec{\mathbf{q}}$ is

$$\mathbf{q}^2 = Q^2 + \nu^2 \tag{3}$$

*Electronic address: bodek@pas.rochester.edu
†Electronic address: christy@jlab.org

Q^2 Previous Pub 16< E_x <40 MeV	Ref	Q^2 Previous Pub QE region	Ref.	This analysis Q^2 Center	Q^2 low	Q^2 high	Comment
				0	0	0	photoabsorption
				0.010	0.003	0.017	
0.0216-0.0194	[8]			0.020	0.017	0.023	
0.0279-0.0251	[8]			0.026	0.023	0.035	
0.0425-0.0382	[8]			0.040	0.035	0.045	
0.0593-0.0532	[8]			0.056	0.045	0.065	
,				0.075	0.065	0.085	
' 0.0973-0.0872	[8]	0.089-0.070	[6, 7]	0.091	0.0110	0.120	
		0.144-0.100	[6, 7]	0.134	0.120	0.160	
				0.190	0.160	0.220	
				0.240	0.220	0.260	
		0.322-0.209	[6, 7]	0.285	0.260	0.320	
				0.350	0.320	0.400	
				0.500	0.400	0.600	
				0.700	0.600	0.800	
				1.000	0.800	1.200	

TABLE I: A summery of the bins in Q^2 (in GeV^2). Also shown are the kinematic range of previous measurements[6–8].

Here M the average nucleon mass and $\nu = E_0 - E'$. In these expressions we have neglected the electron mass which is negligible for the kinematics studied.

For scattering from a nuclear target such as carbon, the excitation energy $E_x = \nu - \nu_{elastic}$ or

$$\nu_{elastic} = E_0 - \frac{E_0}{1 + 2E_0 \sin^2\frac{\theta}{2}/M_A}. \quad (4)$$

where, M_A is the mass of the nuclear target (for carbon $M_{A=12}$=11.178 GeV). Or equivalently

$$E_x = \nu - \frac{Q^2_{elastic}}{2M_A} \quad (5)$$

where $Q^2_{elastic}$ is Q^2 for elastic scattering from a carbon nucleus for incident energy E_0 and scattering angle θ.

A. Description in terms of longitudinal and transverse virtual photon cross sections

This description is most often used in the resonance region. In the one-photon-exchange approximation, the spin-averaged cross section for inclusive electron-proton scattering can be expressed in terms of the photon helicity coupling as

$$\frac{d\sigma}{d\Omega dE'} = \Gamma \left[\sigma_T(W^2, Q^2) + \epsilon\sigma_L(W^2, Q^2)\right], \quad (6)$$

where σ_T (σ_L) is the cross section for photo-absorption of purely transverse (longitudinal) polarized photons,

$$\Gamma = \frac{\alpha E^{'}(W^2 - M_N^2)}{(2\pi)^2 Q^2 M E_0 (1-\epsilon)} \quad (7)$$

is the flux of virtual photons, $\alpha = 1/137$ is the fine structure constant, and

$$\epsilon = \left[1 + 2(1 + \frac{\nu^2}{Q^2})\tan^2\frac{\theta}{2}\right]^{-1} \quad (8)$$

is the relative flux of longitudinal virtual photons (sometimes referred to as the virtual photon polarization). Since Γ and ϵ are purely kinematic factors, it is convenient to define the reduced cross section

$$\sigma_r = \frac{1}{\Gamma}\frac{d\sigma}{d\Omega dE'} = \sigma_T(W^2, Q^2) + \epsilon\sigma_L(W^2, Q^2). \quad (9)$$

All the hadronic structure information is therefore, contained in σ_T and σ_L, which are only dependent on W^2 and Q^2. In the $Q^2 = 0$ limit $\sigma_T(\nu, Q^2)$ should be equal to the measured photoabsorption cross section[9–13] $\sigma_\gamma(\nu)$ for real photons (where ν is the energy of the photon).

B. Description in terms of structure functions

This description is primarily used in the inelastic continuum region. In the one-photon-exchange approximation, the spin-averaged cross section for inclusive electron-proton scattering can be expressed in terms of two structure functions as follows

$$\begin{aligned} \frac{d\sigma}{d\Omega dE'} &= \sigma_M[\mathcal{W}_2(W^2, Q^2) + 2\tan^2(\theta/2)\mathcal{W}_1(W^2, Q^2)] \\ \sigma_M &= \frac{\alpha^2\cos^2(\theta/2)}{[2E\sin^2(\theta/2)]^2} = \frac{4\alpha^2 E'^2}{Q^4}\cos^2(\theta/2) \end{aligned} \quad (10)$$

where σ_M is the Mott cross section, $\alpha = 1/137$ is the fine structure constant. The $\mathcal{F}_1$ and $\mathcal{F}_2$ structure functions are related to $\mathcal{W}_1$ and $\mathcal{W}_2$ by $\mathcal{F}_1 = M\mathcal{W}_1$ and $\mathcal{F}_2 = \nu\mathcal{W}_2$. The structure functions are typically expressed

as functions of Q^2 and W^2 (or alternatively ν or $x = Q^2/(2M\nu)$.

The quantity R is defined as the ratio of the virtual photo-absorption cross section σ_L/σ_T, and is related to the structure functions by,

$$R(x,Q^2) = \frac{\sigma_L}{\sigma_T} = \frac{\mathcal{F}_2}{2x\mathcal{F}_1}(1+\frac{4M^2x^2}{Q^2}) - 1 = \frac{\mathcal{F}_L}{2x\mathcal{F}_1}, \quad (11)$$

where $\mathcal{F}_L$ is called the longitudinal structure function.

where $\mathcal{F}_L$ is called the longitudinal structure function. The structure functions are expressed in terms of σ_L and σ_T as follows:

$$K = \frac{Q^2(1-x)}{2Mx} = \frac{2M\nu - Q^2}{2M} \quad (12)$$

$$\mathcal{F}_1 = \frac{MK}{4\pi^2\alpha}\sigma_T \quad (13)$$

$$\mathcal{F}_2 = \frac{\nu K(\sigma_L+\sigma_T)}{4\pi^2\alpha(1+\frac{Q^2}{4M^2x^2})} \quad (14)$$

$$\mathcal{F}_L(x,Q^2) = \mathcal{F}_2\left(1+\frac{4M^2x^2}{Q^2}\right) - 2x\mathcal{F}_1, \quad (15)$$

or

$$2x\mathcal{F}_1 = \mathcal{F}_2\left(1+\frac{4M^2x^2}{Q^2}\right) - \mathcal{F}_L(x,Q^2). \quad (16)$$

In addition, $2x\mathcal{F}_1$ is given by

$$2x\mathcal{F}_1(x,Q^2) = \mathcal{F}_2(x,Q^2)\frac{1+4M^2x^2/Q^2}{1+R(x,Q^2)}, \quad (17)$$

or equivalently

$$\mathcal{W}_1(x,Q^2) = \mathcal{W}_2(x,Q^2)\times\frac{1+\nu^2/Q^2}{1+R(x,Q^2)}. \quad (18)$$

C. Description in terms of response functions

This description is primarily used in the nuclear excitation and QE peak regions. The electron scattering differential cross section is written in terms of longitudinal ($\mathcal{R}_L(Q^2,\nu)$) and transverse ($\mathcal{R}_T(Q^2,\nu)$) nuclear response functions [14]

$$\frac{d\sigma}{d\nu d\Omega} = \sigma_M[A\mathcal{R}_L(Q^2,\nu) + B\mathcal{R}_T(Q^2,\nu)] \quad (19)$$

where σ_M is the Mott cross section, $A = (Q^2/\mathbf{q}^2)^2$ and $B = \tan^2(\theta/2) + Q^2/2\mathbf{q}^2$.

The relationships between the nuclear response functions, structure functions and virtual photon absorption cross sections are:

$$\mathcal{R}_T(\mathbf{q},\nu) = \frac{2\mathcal{F}_1(\mathbf{q},\nu)}{M} = \frac{K}{2\pi^2\alpha}\sigma_T \quad (20)$$

$$\mathcal{R}_L(\mathbf{q},\nu) = \frac{\mathbf{q}^2}{Q^2}\frac{\mathcal{F}_L(\mathbf{q},\nu)}{2Mx} = \frac{\mathbf{q}^2}{Q^2}\frac{K}{4\pi^2\alpha}\sigma_L \quad (21)$$

Where the units of $\mathcal{R}_L(\mathbf{q},\nu)$ and $\mathcal{R}_T(\mathbf{q},\nu)$ correspond to the units of M^{-1}.

The quantity R (the ratio of the virtual photo-absorption cross section σ_L/σ_T) is related to the response functions by,

$$R(x,Q^2) = \frac{\sigma_L}{\sigma_T} = \frac{\mathcal{F}_L}{2x\mathcal{F}_1} = \frac{2Q^2}{\mathbf{q}^2}\frac{\mathcal{R}_L(\mathbf{q},\nu)}{\mathcal{R}_T(\mathbf{q},\nu)} \quad (22)$$

The square of the electric and magnetic form factors for elastic scattering and nuclear excitations are obtained by the integration of the measured response functions over ν for each nuclear state. When form factors for *nuclear elastic scattering* and *nuclear excitations* are extracted from electron scattering data typically there is an additional factor of Z^2 in the definition of σ_M (where Z is the atomic number of the nucleus). However, in this paper, we treat Quasielastic scattering and nuclear excitations in the same way. Therefore, we do not include a Z^2 factor in the definition of σ_M.

1. Photo-absorption response function

At $Q^2 = 0$ the virtual photoabsorption cross section is equal to the real photoabsoprtion cross section. Therefore, the transverse response function for $Q^2 = 0$ is given by:

$$\mathcal{R}_T(\nu, Q^2=0) = \frac{\nu}{2\pi^2\alpha}\sigma_\gamma(\nu) \quad (23)$$

where $\sigma_\gamma(\nu)$ is the photoabsorption cross section for photons of energy ν on a carbon nucleus.

The measured photoabsorption cross section[9–13] for real photons as a function if photon energy ν from 0 to 2.6 GeV is shown in Fig.1. The photoabsortion cross section as a function of ν from 0 to 0.16 GeV is shown on the top panel of Fig.2. The response function $\mathcal{R}_T(Q^2=0,\nu)$ extracted from the photoabsorption cross section is shown on the bottom panel.

D. Experimental extraction of response functions

The method[6, 7] used to separate $\mathcal{R}_L(Q^2,\nu)$ and $\mathcal{R}_T(Q^2,\nu)$ is described below. The quantity

$$\Sigma(Q^2,\nu) = H\frac{d\sigma}{d\nu d\Omega} \quad (24)$$

$$= \epsilon\mathcal{R}_L(Q^2,\nu) + \frac{1}{2}(\frac{\mathbf{q}}{Q})^2\mathcal{R}_T(Q^2,\nu)$$

$$H = [\frac{1}{\sigma_M}\epsilon(\frac{\mathbf{q}}{Q})^4]$$

$$= \frac{\mathbf{q}^4}{4\alpha^2E'^2}\frac{1}{\cos^2(\theta/2) + 2(\frac{\mathbf{q}}{Q})^2\sin^2(\theta/2)} \quad (25)$$

is plotted as a function of the virtual photon polarization ϵ. The virtual photon polarization ϵ varies from 0 to 1

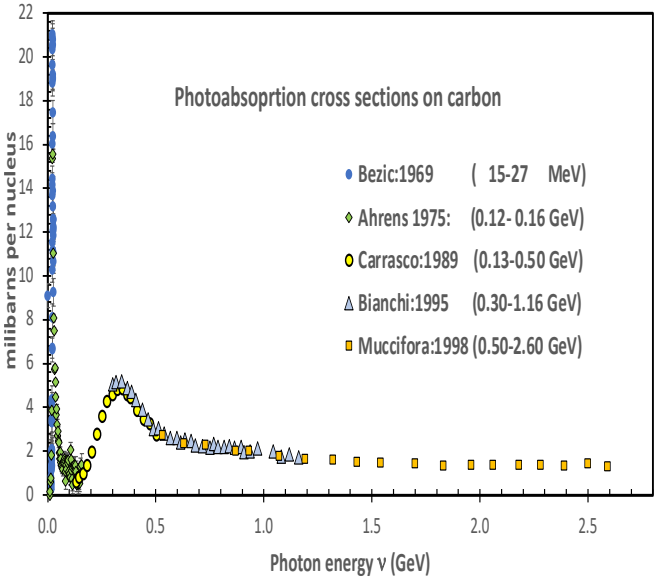

FIG. 1: Photoabsorption cross section as a function of photon energy ν from 0 to 2.6 GeV.

as the scattering angle θ ranges from 180 to 0 degrees. We use equation 25 for H because it is valid for all scattering angles including 180 degrees. Here, $\mathcal{R}_L(Q^2,\nu)$ is the slope, and $\frac{1}{2}\frac{\mathbf{q}^2}{Q^2_{eff}}\mathcal{R}_T(Q^2,\nu)$ is the intercept of the linear fit, However, in the analysis we also include Coulomb corrections as described below.

III. COULOMB CORRECTIONS

In modeling QE and inelastic (pion production) scattering from bound nucleons, Coulomb corrections to QE and inelastic pion production processes are taken into account using the "Effective Momentum Approximation"(EMA) [15, 16]. The approximation is a simple energy gain/loss method, using a slightly higher incident and scattered electron energies at the vertex than measured in the lab. The effective incident energy is $E_{eff} = E_0 + V_{eff}$, and the effective scattered energy is $E'_{eff} = E' + V_{eff}$.

Assuming a spherical charge distribution in the nucleus (of radius R) the electrostatic potential inside the charged sphere can be defined as followed:

$$V(r) = \frac{3\alpha(Z-1)}{2R} + \frac{\alpha(Z-1)}{2R}\frac{r}{R} \tag{26}$$

where R (in units of GeV) is given by:

$$R = 1.1A^{(1/3)} + 0.86A^{(-1/3)}. \tag{27}$$

$$\begin{aligned} V_{eff} &= +0.775V(r=0) \\ &= 0.775\ \frac{3}{2}\ \alpha(Z-1)/R \end{aligned} \tag{28}$$

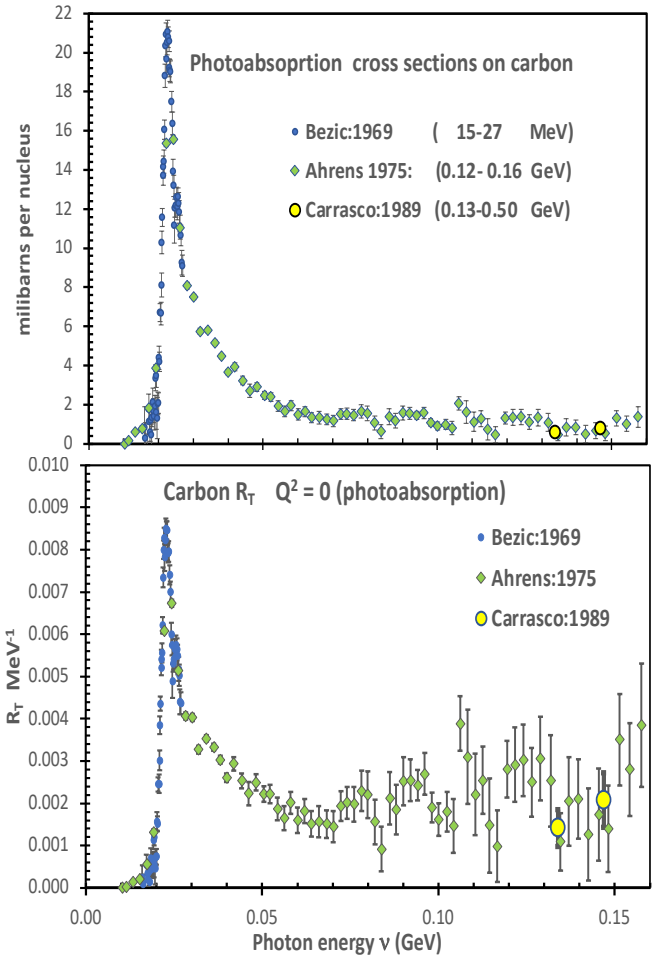

FIG. 2: Top: Photoabsorption cross section as a function of photon energy ν from 0 to 0.16 GeV. Bottom: The response function $\mathcal{R}_T(Q^2=0,\nu)$ extracted from the photon cross sections.

where Z and A are the atomic number and atomic weight of the nucleus, respectively. This value for V_{eff} is consistent with value of $V_{eff} = 3.1 \pm 0.25$ extracted from a comparison of positron and electron QE scattering cross sections on carbon[16]. Here,

$$\begin{aligned} E_{0,eff} &= E_0 + V_{eff} && (29)\\ E'_{eff} &= E' + V_{eff} && (30)\\ \nu_{eff} &= \nu && (31)\\ Q^2_{eff} &= 4(E_0+V_{eff})(E'+V_{eff})\sin^2(\theta/2) && (32)\\ \mathbf{q_{eff}}^2 &= Q^2_{eff} + \nu^2 && (33)\\ W^2_{eff} &= M^2 + 2M\nu - Q^2 eff && (34) \end{aligned}$$

The response functions are calculated with $Q^2 = Q^2_{eff}$ and $E' = E'_{eff}$. In addition, there is a focusing factor $F^2_{foc} = \left[\frac{E_0+V_{eff}}{E_0}\right]^2$ which modifies the Mott cross section. The modified Mott cross section is

$$\sigma_{M-eff} = F^2_{foc}\frac{\alpha^2\cos^2(\theta/2)}{[2E_{eff}\sin^2(\theta/2)]^2}$$

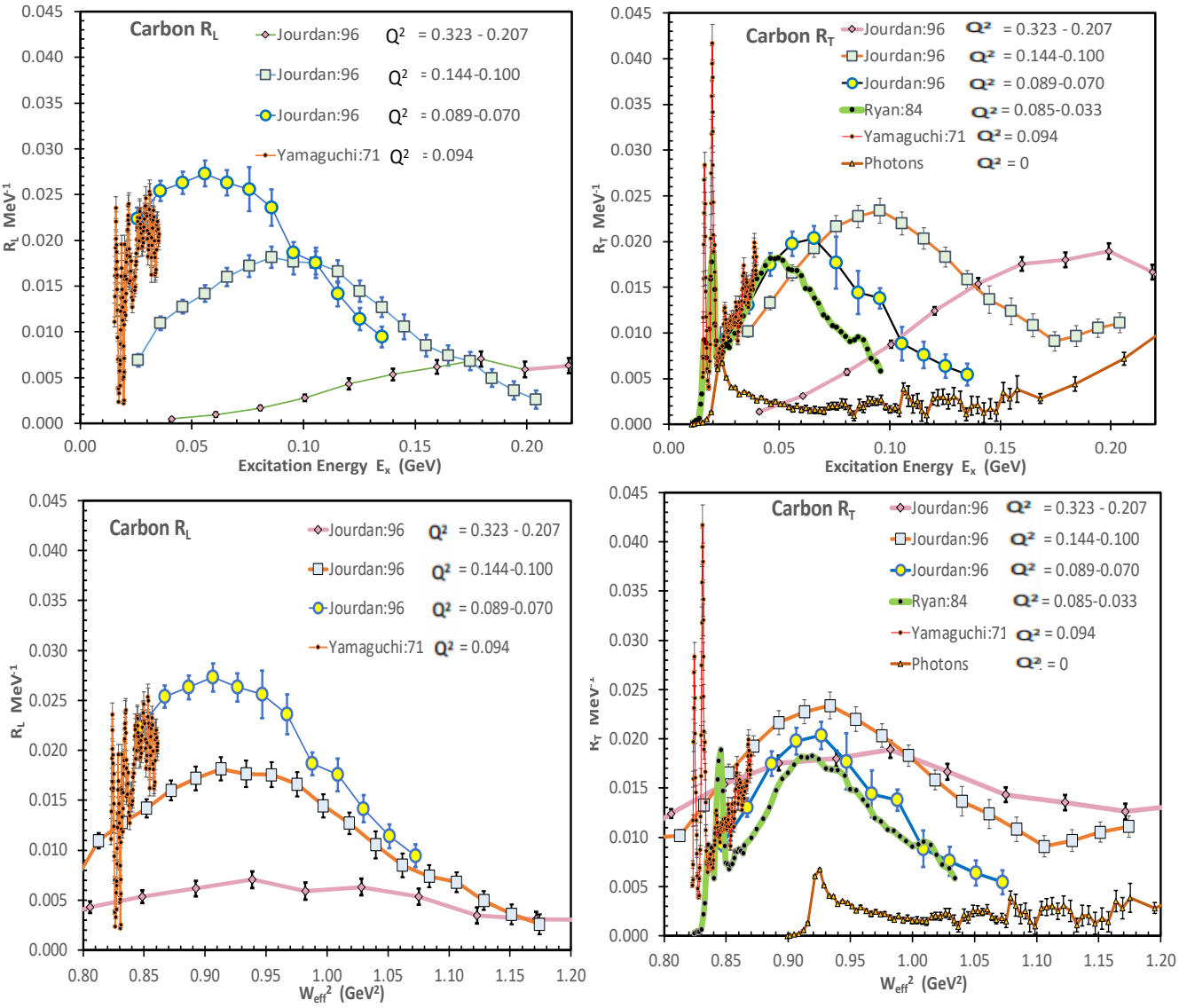

FIG. 3: Top: $\mathcal{R}_L(Q^2_{eff},\nu)$ ANS $\mathcal{R}_T(Q^2_{eff},\nu)$ for various values of Q^2_{eff} as a function of excitation energy E_x. Bottom: Same as the top panel, but versus W^2. Shown are the three published RL_RT extractions bu Jourdan in 1996 in the QE region and in of Rl/RT extractions by Yamaguchi in 1996. For the R_T plot we also show the R_T extracted from the 0.1506 GeV and 180 degrees data of Ryan:1984 and R_T extracted from Photoabsorption data (Q^2=0) It is clear that the Q^2 bin entering corrections are minimized if the analysis is done in bins of E_x for E_x <0.040 GeV. For E_x >0.040 GeV the Q^2 bin centering corrections are minimized if the analysis is done in in bins of W^2.

Therefore

$$\epsilon^{CC} = \left[1+2(1+\frac{\nu^2}{Q^2_{eff}})\tan^2\frac{\theta}{2}\right]^{-1} \quad (35)$$

$$\Sigma'(Q^2_{eff},\nu) = H_{CC}\frac{d\sigma}{d\nu d\Omega} \quad (36)$$

$$H^{cc} = \left[\frac{E_0}{E_0+V_{eff}}\right]^2 \times \frac{\mathbf{q_{eff}}^4}{4\alpha^2 E'^2_{eff}} \frac{1}{\cos^2(\theta/2)+2(\frac{\mathbf{q_{eff}}}{Q_{eff}})^2\sin^2(\theta/2)} \quad (37)$$

In this analysis correction factors are determined using an overall fit to model all existing electron scattering data on ^{12}C. The fit includes the following components: (a) Nuclear-elastic scattering and excitation of nuclear states, (b) Quasielastic scattering and (c) Resonance production and the inelastic continuum. The parameterizations of the form factors for nuclear-elastic scattering and excitation of nuclear states are presented in [17]. A brief description of the quasielastic and resonance production fits and the measurement of the Coulomb Sum Rule are presented in [18].

As described below, we bin the data in Q^2_{eff} and ν

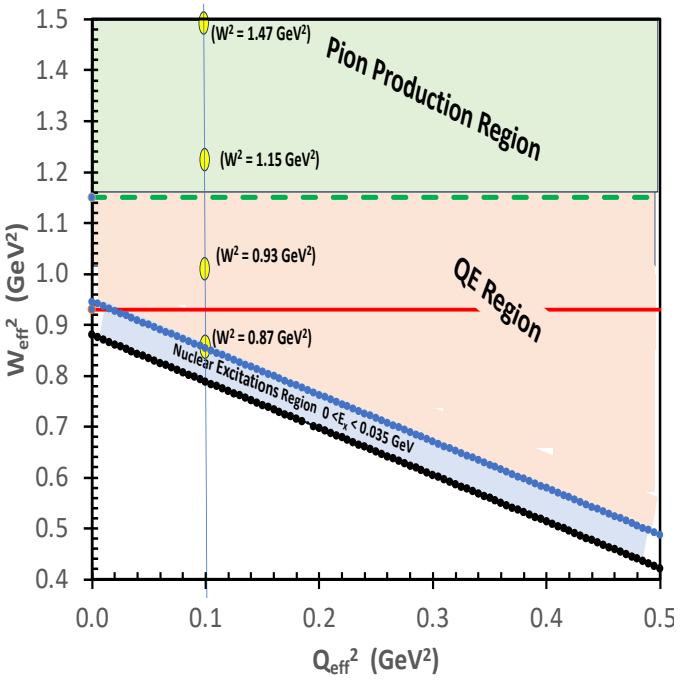

FIG. 4: W^2 regions.

bins. We apply bin centering corrections as well as normalization corrections to each data set to account for the small difference in the normalizations (within the quoted errors) of each data set. We then perform a (Rosenbluth) linear fit for for the data in each bin in ν. Here, $\mathcal{R}_L(Q^2_{eff},\nu)$ is the slope, and $\frac{1}{2}\frac{\mathbf{q_{eff}}^2}{Q^2_{eff}}\mathcal{R}_T(Q^2_{eff},\nu)$ is the intercept of the linear fit,

A. Summary of corrections to the data

We use our cross section fit (σ_{model}) to evaluate the following corrections to the cross sections in each bin in Q^2.

1. From the overall fit we extract the relative normalization (N_i) of the various data sets.

2. We use the fit to apply Q^2 bin centering corrections (C_i) to all extracted value off Σ'_i that are within the Q^2_{eff} range for each Q^2_{eff} bin. The bin centering corrections is done by only changing Q^2 and keeping the same values of W^2.

$$C_i = \frac{\epsilon\mathcal{R}_L^{fit}(Q^2_{center}) + \frac{1}{2}(\frac{\mathbf{q_{center}}}{Q_{center}})^2\mathcal{R}_T^{fit}(Q^2_{center})}{\epsilon\mathcal{R}_L^{fit}(Q^2_{eff}) + \frac{1}{2}(\frac{\mathbf{q_{eff}}}{Q_{eff}})^2\mathcal{R}_T^{fit}(Q^2_{eff})}.$$

After the application of the bin centering corrections to all extracted values Σ'_i in each Q^2_{eff} bin we can assume that extracted values of Σ_i are at Q^2_{center}. When we apply these corrections, we keep the final state invariant

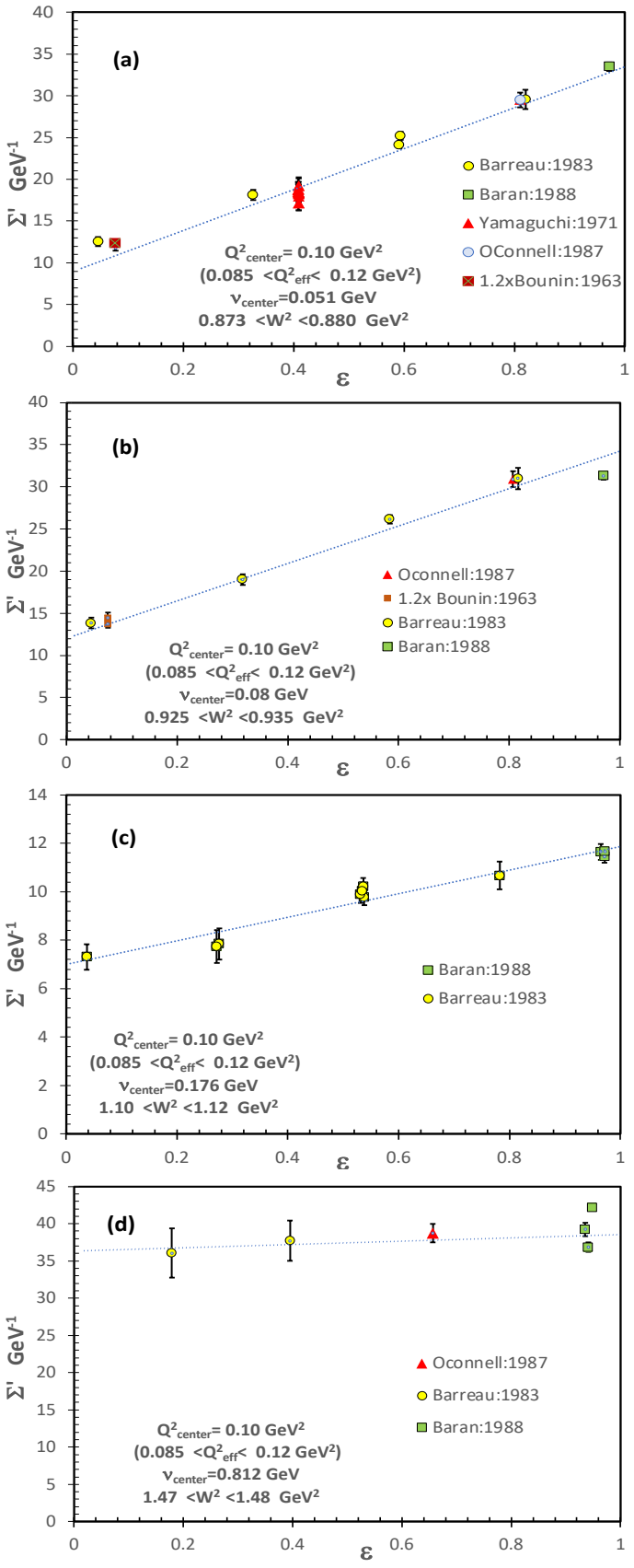

FIG. 5: Sample RL RT plots.

mass W^2 fixed for $\nu > 30$ MeV, and only correct for the change in Q^2_{eff}. For $\nu < 30$ MeV we use the excitation energy E_X instead of W^2.

B. Electron scattering at 180^o

The response function $\mathcal{R}_T(Q^2_{eff},\nu)$ can also be extracted directly from electron scattering data at 180^o.

$$\mathcal{R}_T(Q^2_{eff},\nu) \;=\; \big[\frac{E_0}{E_0+V_{eff}}\big]^2 \times \frac{{Q_{eff}}^4}{4\alpha^2 E'^2_{eff}}\frac{d\sigma}{d\nu d\Omega} \quad (38)$$

C. Q^2 versus q

The values of the response function then can be plotted versus W^2 or versus ν (or E_x) that corresponds to the the centered value Q^2_{center} using expression:

$$\begin{aligned} \nu^{center} &= (W^2 - M^2 + Q^2_{center})/2M \\ E_x^{center} &= \nu^{center} - Q^2_{center}/2M_A \end{aligned} \quad (39)$$

In previous analyses the extraction of the response functions done for fixed value of $\mathbf{q_{eff}}$. However, it is more convenient to do the extraction in bins of Q^2_{eff}. This is because for fixed Q^2_{eff} the peak position of the quasielastic distribution is at same value of both W^2 (and ν) for all scattering angles. In contrast, for fixed value of $\mathbf{q_{eff}}$ the the peak position of the quasielastic distribution in ν depends on the scattering angle.

$$\nu = (W^2 - M^2 + \mathbf{q}_{center} - \nu^2)/2M$$

Similarly, at fixed Q^2 each nuclear state with excitation energy E_x is at the same value of ν at all scattering angles.

In addition to binning the data in Q^2 it is also more convenient to extract the response function in bins of W^2 in the quasielastic region, and in bins of excitation energy E_x at low values of W^2 near threshold.

A Elastic electron-nucleon scattering

In the case of elastic scattering from free nucleons ($x = Q^2/2M\nu$=1) the structure functions are related to the nucleon form factors by the following expressions:

$$\mathcal{W}^{elastic}_{1p} = \delta(\nu - \frac{Q^2}{2M})\tau|G_{Mp}(Q^2)|^2$$

$$\mathcal{W}^{elastic}_{1n} = \delta(\nu - \frac{Q^2}{2M})\tau|G_{Mn}(Q^2)|^2$$

and

$$\begin{aligned} \mathcal{W}^{elastic}_{2p} &= \delta(\nu - \frac{Q^2}{2M})\frac{[G_{Ep}(Q^2)]^2 + \tau[G_{Mp}(Q^2)]^2}{1+\tau} \\ \mathcal{W}^{elastic}_{2n} &= \delta(\nu - \frac{Q^2}{2M})\frac{[G_{En}(Q^2)]^2 + \tau[G_{Mn}(Q^2)]^2}{1+\tau} \end{aligned}$$

$$R^{elastic}_{p,n}(x=1,Q^2) = \frac{\sigma^{elastic}_L}{\sigma^{elastic}_T} = \frac{4M^2}{Q^2}\left(\frac{G^2_E}{G^2_M}\right)$$

Here, $\tau = Q^2/4M^2_{p,n}$, where $M_{p,n}$ are the masses of proton and neutron. Therefore, G_{Mp} and G_{Mn} contribute to the transverse virtual photo-absorption cross section, and G_{Ep} and G_{En} contribute to the longitudinal cross section. The elastic response functions for the proton are given by The relationship between the nuclear response functions, and structure functions is

$$\begin{aligned} \mathcal{R}_T(\mathbf{q},\nu) &= 2\tau[G_{Mp}(Q^2)]^2 = \frac{Q^2}{2M^2_p}[G_{Mp}(Q^2)]^2 \\ \mathcal{R}_L(\mathbf{q},\nu) &= \frac{\mathbf{q^2}}{Q^2}[G_{Ep}(Q^2)]^2 \end{aligned} \quad (40)$$

Appendix A SUMMARY OF CROSS SECTION DATA

Appendix B NOTE TO ZIGGY

[1] B. Mihaila and J. Heisenberg, Phys. Rev. Lett. **84**, 1403 (2000), arXiv:nucl-th/9910007 .
[2] A. Lovato, S. Gandolfi, J. Carlson, S. C. Pieper, and R. Schiavilla, Phys. Rev. Lett. **117**, 082501 (2016), arXiv:1605.00248 [nucl-th] .
[3] I. C. Cloët, W. Bentz, and A. W. Thomas, Phys. Rev. Lett. **116**, 032701 (2016), arXiv:1506.05875 [nucl-th] .
[4] T. Franco-Munoz, R. González-Jiménez, and J. M. Udias, "Effects of two-body currents in the one-particle one-hole electromagnetic responses within a relativistic mean-field model," (2022), arXiv:2203.09996 [nucl-th] .
[5] J. E. Sobczyk, B. Acharya, S. Bacca, and G. Hagen, Phys. Rev. C **102**, 064312 (2020), arXiv:2009.01761 [nucl-th] .
[6] J. Jourdan, Nucl. Phys. A **603**, 117 (1996).
[7] J. Jourdan, Phys. Lett. B **353**, 189 (1995).
[8] A. Yamaguchi, T. Terasawa, K. Nakahara, and Y. Torizuka, Phys. Rev. C **3**, 1750 (1971).
[9] N. Bezić, D. Brajnik, D. Jamnik, and G. Kernel, Nucl. Phys. A **128**, 426 (1969).
[10] J. Ahrens *et al.*, Nucl. Phys. A **251**, 479 (1975).
[11] R. C. Carrasco and E. Oset, Nucl. Phys. A **536**, 445 (1992).
[12] N. Bianchi *et al.*, Phys. Rev. C **54**, 1688 (1996).

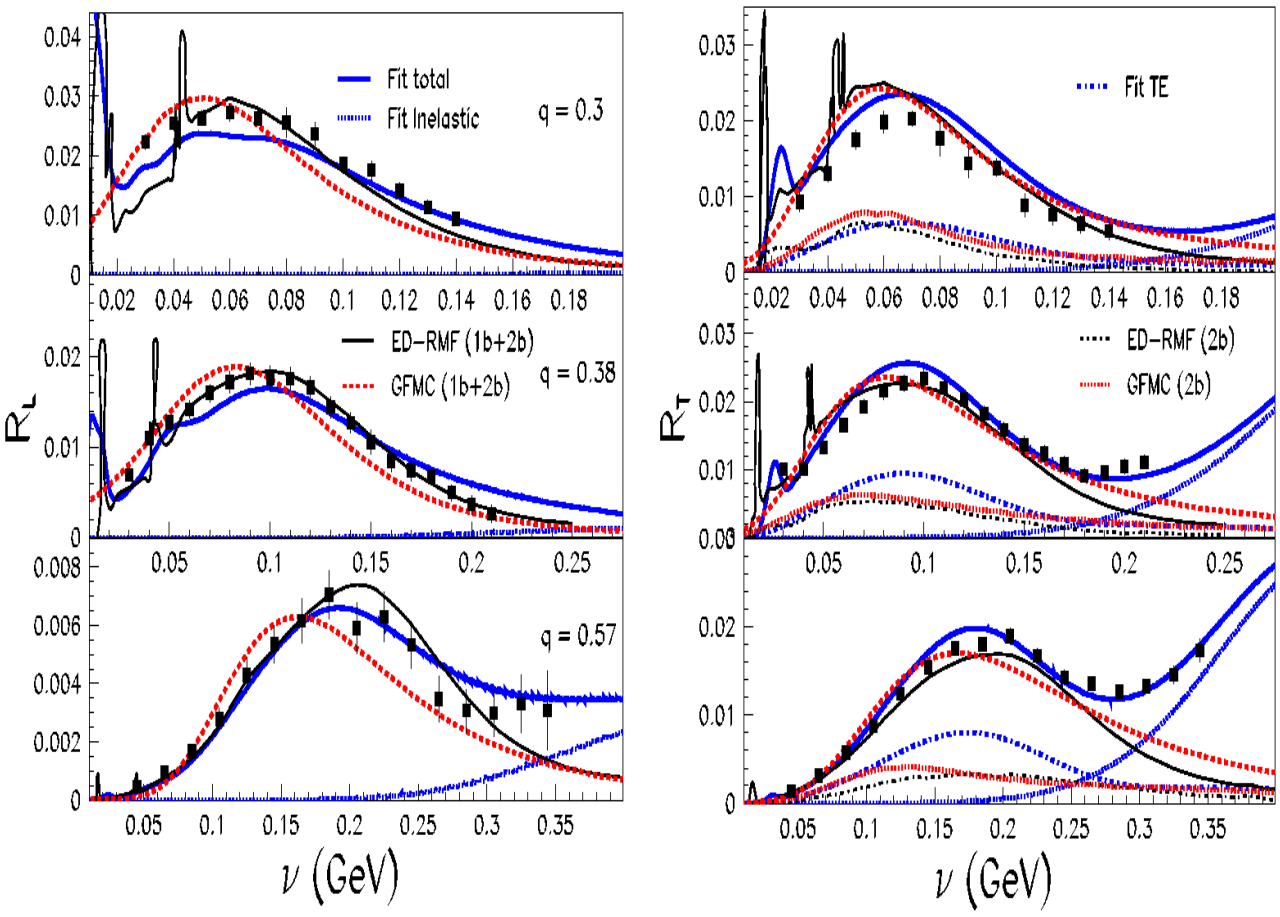

FIG. 6: Comparisons between our extraction of $\mathcal{R}_L(\mathbf{q},\nu)$ and $\mathcal{R}_T(\mathbf{q},\nu)$ (in units of MeV^{-1} and the extraction (for only three values of $\mathbf{q}$) by Jourdan[6, 7]. (The Jourdan analysis includes data from only two experiments). Also shown are comparisons to 1b+2b GFMC[2] and ED-RMF[4] theoretical predictions. In these two models the curves labeled 2b are the only contribution of 2-body currents to $TE(\mathbf{q},\nu)$. The transverse enhancement in both 1b and 2b currents is included in the total.

[13] V. Muccifora *et al.*, Phys. Rev. C **60**, 064616 (1999), arXiv:nucl-ex/9810015 .

[14] J. A. Caballero, M. C. Martinez, J. L. Herraiz, and J. M. Udias, Phys. Lett. B **688**, 250 (2010), arXiv:0912.4356 [nucl-th] .

[15] A. Aste, C. von Arx, and D. Trautmann, Eur. Phys. J. A **26**, 167 (2005), arXiv:nucl-th/0502074 .

[16] P. Gueye *et al.*, Phys. Rev. C **60**, 044308 (1999).

[17] A. Bodek and M. E. Christy, "Contribution of Nuclear Excitation Electromagnetic Form Factors in ^{12}C and ^{16}O to the Coulomb Sum Rule. arXiv: 2301.05650[nucl-th]," (2023), arXiv:2301.05650 [nucl-th] .

[18] A. Bodek and M. E. Christy, Phys. Rev. C **106**, L061305 (2022), arXiv:2208.14772 [hep-ph] .

[19] P. Barreau *et al.*, Nucl. Phys. **A402**, 515 (1983).

[20] J. S. O'Connell *et al.*, Phys. Rev. **C35**, 1063 (1987).

[21] R. M. Sealock *et al.*, Phys. Rev. Lett. **62**, 1350 (1989).

[22] D. T. Baran *et al.*, Phys. Rev. Lett. **61**, 400 (1988).

[23] D. S. Bagdasaryan *et al.*, "Measurement of the spectra of (e,e') scattering ^{9}Be and ^{12}C nuclei in the inelastic region at q^2 approximately 0.4 (gev/c)^2," (1988), yERPHI-1077-40-88.

[24] M. Murphy *et al.*, Phys. Rev. C **100**, 054606 (2019), arXiv:1908.01802 [hep-ex] .

[25] J. Arrington *et al.*, Phys. Rev. **C53**, 2248 (1996), nucl-ex/9504003 .

[26] D. B. Day *et al.*, Phys. Rev. **C48**, 1849 (1993).

[27] J. Arrington *et al.*, Phys. Rev. Lett. **82**, 2056 (1999), nucl-ex/9811008 .

[28] J. Arrington *et al.*, Phys. Rev. C **104**, 065203 (2021), arXiv:2110.08399 [nucl-ex] .

[29] J. Seely *et al.*, Phys. Rev. Lett. **103**, 202301 (2009), arXiv:0904.4448 [nucl-ex] .

[30] R. R. Whitney, I. Sick, J. R. Ficenec, R. D. Kephart, and W. P. Trower, Phys. Rev. C **9**, 2230 (1974).

[31] S. Alsalmi *et al.*, "Experimental investigation of the structure functions of ^{12}c in the resonance region," (2023), to be published.

[32] I. Albayrak *et al.*, "Precise measurements of electron scattering quasielastic cross sections on ^{12}c," (2023), to be published.

[33] S. A. Alsalmi, *Measurement of the Nuclear Dependence of F_2 and R=Sigma_L/Sigma_T in The Nucleon Resonance Region*, Ph.D. thesis, Kent State University, Kent State U. (2019).

[34] J. Gomez *et al.*, Phys. Rev. D **49**, 4348 (1994).

	Data Set	Q^2_{Min} (GeV^2)	Q^2_{Max} (GeV^2)	# Data Points	Normalization	Error
1	Barreau83 [19]				0.99185	
2	O'Connell87 [20]				0.97869	
3	Sealock89 [21]				1.0315	
4	Baran88 [22]				0.99241	
5	Bagdasaryan88 [23]				0.98777	
6	Dai19 [24]				1.0108	
7	Arrington96[25]				0.97427	
8	Day93 [26]				1.0071	
9	Arrington99 [27]				0.98884	
10	Gaskell21 [28, 29]				0.99340	
11	Whitney74 [30, 45]				1.0149	
12	E04-001-2005 (preliminary) [31–33]				0.99812	
13	E04-001-2007 (preliminary) [31–33]				1.0029	
14	Gomez74 [34, 35]				1.0125	
15	Fomin10 [36, 37]				1.0046	
16	Yamaguchi71 [8]				1.0019	
17	Ryan84 [38]				1.0517	
18	Bounin63 [39, 40]				1.2	0.1
19	Czyk63 [41]				1.6	0.2
20	Photo-Daphne				1.00	
21	Spamer70 [8, 42]				1.0	
22	Goldemberg64 [43]				1.0	
23	dForrest65 [8, 44]				1.0	
	Zeller73 [46] (not used)					

TABLE II: A summary table of the ^{12}C data sets used in the universal fit. Shown are the number of data points, the Q^2 range of each set, the normalization factor, and the universal fit χ^2 per degree of freedom for each set. The Zeller73 [46] data set is inconsistent with all other data sets and is not used.

[35] "Resonance Data Archive at Jefferson Lab Hall C," Https://hallcweb.jlab.org/resdata/.

[36] N. Fomin *et al.*, Phys. Rev. Lett. **105**, 212502 (2010), arXiv:1008.2713 [nucl-ex] .

[37] Y. Liang *et al.* (Jefferson Lab Hall C E94-110), Phys. Rev. C **105**, 065205 (2022), arXiv:nucl-ex/0410027 .

[38] P. J. Ryan, J. B. Flanz, R. S. Hicks, B. Parker, and G. A. Peterson, Phys. Rev. C **29**, 655 (1984).

[39] P. Bounin and J. R. Bishop, J. Phys, **24**, 974 (1963).

[40] J. Lovseth, Nuovo Cim. A **57**, 382 (1968).

[41] W. Czyz, Phys. Rev. **131**, 2141 (1963).

[42] P. Antony-Spies, P. P. Delsanto, E. Spamer, A. Goldman, and O. Titze, Phys. Lett. B **31**, 632 (1970).

[43] J. Goldemberg and W. C. Barber, Phys. Rev. **134**, B963 (1964).

[44] T. Deforest, J. Walecka, G. Vanpraet, and W. Barber, Physics Letters **16**, 311 (1965).

[45] E. J. Moniz, I. Sick, R. R. Whitney, J. R. Ficenec, R. D. Kephart, and W. P. Trower, Phys. Rev. Lett. **26**, 445 (1971).

[46] D. Zeller, *Investigation of the structure of the C-12 nucleus by high-energy electron scattering (DESY-F23-73-2)*, Master's thesis, University of Karlsruhe (1973).